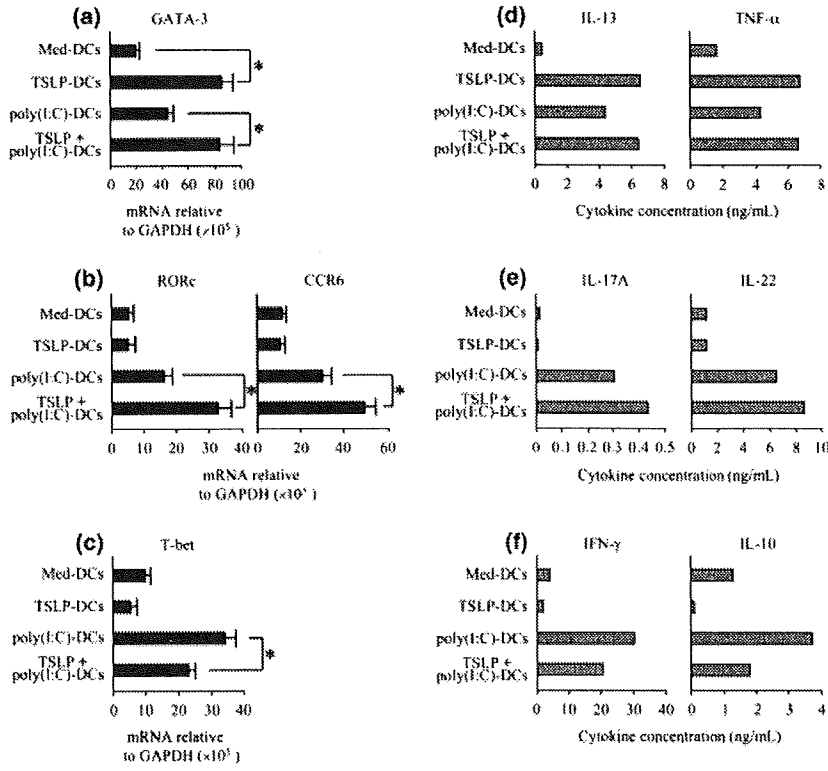


Fig. 4. TSLP+poly(I : C)-activated DCs primed naïve $CD4^+$ T cells to produce IL-17 and IL-22, but failed to induce further development of the inflammatory Th2 cells. Naïve $CD4^+$ T cells were primed for 7 days by DCs activated with TSLP, poly(I : C), or the combination of both stimuli. (a–c), Expression levels of mRNA encoding GATA-3 (a), RORc and CCR6 (b), and T-bet (c). Expression levels were measured using real-time quantitative RT-PCR. Closed bar and vertical error bars indicate the mean and SD of five independent experiments, respectively. Student's *t*-test for unpaired data was used to compare the values between two groups. $^*P<0.05$. (d–f), Cytokine production of primed T cells. After 7 days of co-culture, T cells were restimulated for 24 h with anti-CD3 and anti-CD28 mAbs. IL-13 and TNF-α (d), IL-17A, and IL-22 (e), and IFN-γ and IL-10 (c), were measured in the culture supernatant using protein ELISA. Data represent one of five independent experiments. TSLP, thymic stromal lymphopoietin; DCs, dendritic cells.

(Fig. 5c, right panels). These findings suggest that TSLP+poly(I : C)-DCs may induce conversion of Th17/Th1 cells to Th17 cells.

### *TSLP can directly prime human memory $CD4^+$ T cells to enhance the production of Th17 cytokines*

Although freshly isolated peripheral blood human $CD4^+$ T cells do not show any response to TSLP, we recently found that TCR stimulation allows a potent response of $CD4^+$ T cells to TSLP and that TSLP can directly enhance T cell expansion [37, 38]. To examine the possibility that the direct action of TSLP on $CD4^+$ T cells is involved in differentiation of Th17 cells, purified naïve $CD4^+CD45RA^+$ T cells and memory $CD4^+CD45RA^-$ T cells were activated with Th17-cell differentiation media, anti-CD3, and anti-CD28 with neutralizing Abs for IL-4, and IFN-γ with or without IL-6 and IL-23, in the presence or absence of TSLP. After 3 days of culture, cells were further expanded for 4 days with IL-2, and the production of IL-17 and IL-22 was measured in the culture supernatant using protein ELISA. TSLP had no effect on IL-17 or IL-22 production of naïve $CD4^+CD45RA^+$ T cells cultured even in Th17-cell differentiation media (Fig. 6). However, TSLP significantly enhanced IL-17 and IL-22 production of memory $CD4^+CD45RA^-$ T cells in Th17-cell differentiation media. These data suggest that in addition to indirectly priming naïve $CD4^+$ T cells to differentiate into Th17 cells with a memory phenotype, TSLP may also directly act on these memory T cells to accelerate further expansion and production of IL-17.

## Discussion

In the present study, we demonstrated for the first time that TSLP and TLR3 ligands activated human blood $CD11^+$ DCs to produce more IL-23 and more programmed naïve $CD4^+$ T cells to differentiate into Th17 cells compared with the TLR3 ligand alone, and a combination of TSLP and TLR3 ligands did not alter development of the inflammatory Th2 cells compared with TSLP alone. These results suggest that through DC activation, human TSLP

 

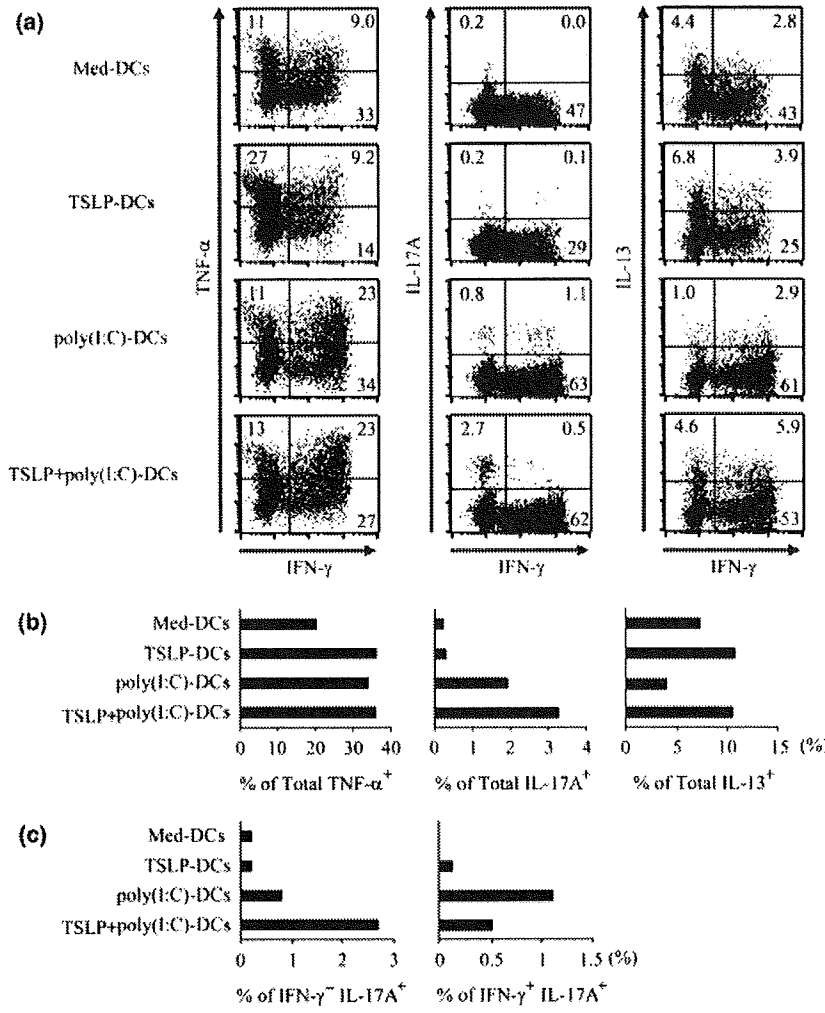


Fig. 5. TSLP+poly(I : C)-DCs reduced IL-17 and IFN-γ double-producing T cells and increased IL-17 single-producing T cells. $CD11c^+$ DCs cultured with TSLP, poly(I : C), a combination of both stimuli, or medium alone were used to prime naïve $CD4^+$ T cells. After 7 days of co-culture, T cells were restimulated for 6 h with PMA plus ionomycin, and production of indicated T cell-derived cytokines was determined by intracellular cytokine staining. (a), Dot blots profiles of indicated cytokines. Numbers indicate percent of cells in each quadrant. Data represent one of three independent experiments. (b), Percentage of TNF-α– IL-17–, IL-13 – producing cells. Data represent numbers in (a). (c), Percentage of IL-17 single-producing cells (IFN-γ $IL\text{-}17^+$), and IFN-γ and IL-17 double-producing cells ($IFN\text{-}\gamma^+ IL\text{-}17^+$). Data represents numbers in (a). TSLP, thymic stromal lymphopoietin; DCs, dendritic cells.

and TLR3 ligands promote Th17-cell differentiation under Th2-polarizing conditions. If Th2 cells predominate in driving inflammation in mild asthma, there is evidence that a more severe asthmatic phenotype is regulated through a mixture of Th1 and Th2 cells with neutrophilic inflammation probably induced by Th17 cells in the lungs [26]. TSLP-mediated Th17-cell commitment under Th2-polarizing conditions may be involved in the development of an inflammatory mixture of Th2 and Th17 cells, a unique profile that resembles severe asthma.

In humans, $CD4^+$ memory T cells have been defined as $CD45RO^+CD62L^+CCR7^+$ central memory cells and $CD45RO^+CD62L^-CCR7^-$ effector memory cells by their distinct surface phenotype, homing capacity, and effector functions [39, 40]. These T cell subsets can be further divided into subsets that are prone to produce Th1 or Th2 cytokines according to their differential expression of chemokine and tissue-homing receptors [40–42], linking memory T cell subsets with a polarized Th1 or Th2 function. TSLP-DCs play important roles not only in Th2 priming but also in the maintenance and further polarization of Th2 central memory cells in allergic diseases [5]. In this study, we show that DCs activated by a combination of TSLP and poly(I : C) primed naïve $CD4^+$ T cells to produce IL-17 and IL-22 and priming with TSLP+poly(I : C)-DCs down-regulated CD45RA and up-regulated CD45RO in $CD4^+$ T cells, acquiring a $CD45RA^-CD45RO^+CD62L^+CCR7^+$ central memory T cell phenotype.

 

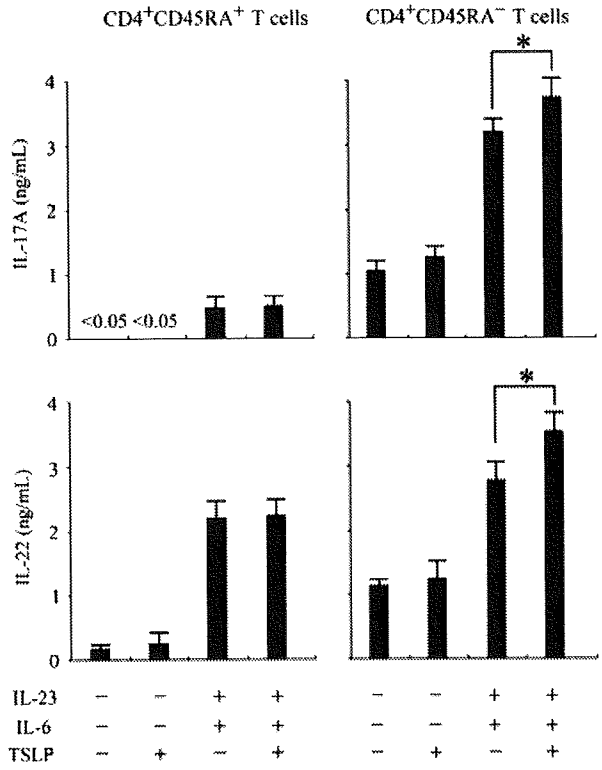


Fig. 6. TSLP directly acted on human memory $CD4^+$ T cells to enhance production of Th17 cytokines. Purified $CD4^+CD45RA^+$ naïve T cells and $CD4^+CD45RA$ memory T cells were cultured with anti-CD3, anti-CD28, anti-IL-4, and anti-IFN-γ Abs in the presence or absence of IL-6 and IL-23 with or without TSLP. After 3 days of culture, cells were further cultured for 4 days with anti-CD3, anti-CD28, and IL-2. Production of IL-17 and IL-22 was measured in the culture supernatant using protein ELISA. Closed bar and horizontal error bars indicate the mean and SD of three independent experiments, respectively. Student's *t*-test for unpaired data was used to compare the values between two groups. $^*P<0.05$. TSLP, thymic stromal lymphopoietin.

Th17 cells are linked to the development of autoimmune diseases *in vivo* [16, 17] and the IL-23–IL-17 axis is involved in human psoriasis and inflammatory bowel diseases, suggesting an important role for Th17 cytokines in chronic inflammatory diseases [17, 18, 22]. Therefore, IL-23-mediated generation of Th17 central memory cells by TSLP+poly(I : C)-DCs may be involved in maintenance of chronic inflammation of allergic diseases.

In addition, restimulation with anti-CD3, anti-CD28 mAbs, and IL-2 rapidly converts TSLP+poly(I : C)-DCs-induced central memory T cells into effector memory T cells highly expressing CCR4 (Fig. 3), suggesting that T cells expanded with TSLP+poly(I : C)-DCs can rapidly acquire effector functions. Thus, through DC activation, TSLP and TLR3 ligands may facilitate the link between differentiation and maturation of naïve, memory, and effector T cells in chronic inflammation of allergic diseases.

Previous studies have reported that TLR3 ligand, virus-derived double-stranded RNA activates bronchial epithelial cells to produce pro-inflammatory mediators, including TSLP [30–32]. In this study, we showed that TSLP and TLR3 ligand stimulation induced strong and unique activation of DCs. In addition, exacerbation of asthmatic inflammation is often triggered by infection involving airway-targeting RNA viruses [27–29], and TSLP expression correlates with disease severity [7, 8]. Therefore, the TLR3 ligand may play dual roles in exacerbation of asthmatic inflammation through induction of TSLP by epithelial cells and activation of DCs in the presence of TSLP.

In human blood, the other unique DC subsets are immature plasmacytoid DCs. Bratke et al. [43] demonstrated that not only human myeloid $CD11c^+$ DCs but also plasmacytoid DCs infiltrate bronchoalveolar lavage fluid in the lung during segmental allergen challenge using allergens such as birch, rye, and *Dermatophagoides pteronyssinus*. We examined whether the TSLP and/or the TLR3 ligand can activate immature plasmacytoid DCs. However, stimulation of the TSLP and/or the TLR3 ligand did not directly induce CD80 up-regulation and IFN-α secretion in immature plasmacytoid DCs (data not shown). In mice, plasmacytoid DCs can differentiate into myeloid DCs after viral infection and poly(I : C) injection to mice through type-I IFN production [44]. Therefore, in humans, TLR3 ligands may play an additional role in exacerbation of asthmatic inflammation indirectly through conversion of plasmacytoid DCs to TSLPR-expressing $CD11c^+$ DCs.

IL-23 consists of a unique p19 subunit coupled to the p40 subunit of IL-12. However, enhanced DC cytokine production by TSLP and poly(I : C) stimulation were demonstrated only in IL-23 and not in IL-12 (Fig. 2a). Using real-time quantitative RT-PCR, we found that priming of DCs with TSLP and poly(I : C) enhanced gene expression of IL-23p19 but not that of IL-12p40 and IL-12p35, another subunit of bioactive IL-12 (data not shown). These data suggest that increased expression of IL-23p19 but not IL-12p35 and IL-12p40 may enhance the production of IL-23 but not of IL-12 in DCs primed with TSLP and poly(I : C).

In conclusion, we demonstrated that TSLP and TLR3 ligands activate human blood $CD11^+$ DCs to produce more IL-23 and program naïve $CD4^+$ T cells more to differentiate into Th17 cells compared with the TLR3 ligand alone, and a combination of TSLP and TLR3 ligands does not alter development of the inflammatory Th2 cells compared with TSLP alone. These results suggest that through DC activation, human TSLP and TLR3 ligands promote Th17-cell differentiation under Th2-polarizing conditions, implying that in allergic diseases, virus-derived double-stranded RNA and TSLP may play a role in Th17 lineage commitment, even under Th2-predominant polarizing conditions.

 

## Acknowledgements

We thank Dr Dovie Wylie and Ms Yoshimi Yamakawa for assistance with preparation of the manuscript. This work was supported by Grants-in-aid for Scientific Research, 17659212, 18012029, 18015028, 18209027, 18590679, and 20390207 from the Ministry of Education, Culture, Sports, Science, and Technology of Japan, a Grant-in-Aid for Research on Measures for Intractable Diseases, and Research on Advanced Medical Technology from the Ministry of Health, Labor, and Welfare, Japan, and a Grant-in-Aid by the Uehara Memorial Foundation, Takeda Science Foundation, Mochida Memorial Foundation for Medical and Pharmaceutical Research, Novartis Foundation for the Promotion of Science, Astellas Foundation for Research on Metabolic Disorders, Yakult Bioscience Research Foundation, and the Naito Foundation. None of the authors have competing interests.

## References

1 Ziegler SF, Liu YJ. Thymic stromal lymphopoietin in normal and pathogenic T cell development and function. *Nat Immunol* 2006; 7:709–14.
2 Liu YJ, Soumelis V, Watanabe N *et al.* TSLP: an epithelial cell cytokine that regulates T cell differentiation by conditioning dendritic cell maturation. *Annu Rev Immunol* 2007; 25:193–219.
3 Soumelis V, Reche PA, Kanzler H *et al.* Human epithelial cells trigger dendritic cell-mediated allergic inflammation by producing TSLP. *Nat Immunol* 2002; 3:673–80.
4 Ito T, Wang YH, Duramad O *et al.* TSLP-activated dendritic cells induce an inflammatory T helper type 2 cell response through OX40 ligand. *J Exp Med* 2005; 202:1213–23.
5 Wang YH, Ito T, Wang YH *et al.* Maintenance and polarization of human $T_H2$ central memory T cells by thymic stromal lymphopoietin-activated dendritic cells. *Immunity* 2006; 24:827–38.
6 Gilliet M, Soumelis V, Watanabe N *et al.* Human dendritic cells activated by TSLP and CD40L induce proallergic cytotoxic T cells. *J Exp Med* 2003; 197:1059–63.
7 Ying S, O'Connor B, Ratoff J *et al.* Thymic stromal lymphopoietin expression is increased in asthmatic airways and correlates with expression of Th2-attracting chemokines and disease severity. *J Immunol* 2005; 174:8183–90.
8 Préfontaine D, Hamid Q. Airway epithelial cells in asthma. *J Allergy Clin Immunol* 2007; 120:1475–8.
9 Liu YJ. Thymic stromal lymphopoietin and OX40 ligand pathway in the initiation of dendritic cell-mediated allergic inflammation. *J Allergy Clin Immunol* 2007; 120:238–44.
10 Barnes PJ. Immunology of asthma and chronic obstructive pulmonary disease. *Nat Rev Immunol* 2008; 8:183–92.
11 Hammad H, Lambrecht BN. Dendritic cells and epithelial cells: linking innate and adaptive immunity in asthma. *Nat Rev Immunol* 2008; 8:193–204.
12 Holgate ST. Pathogenesis of asthma. *Clin Exp Allergy* 2008; 38:872–97.
13 Zhou B, Comeau MR, De Smedt T *et al.* Thymic stromal lymphopoietin as a key initiator of allergic airway inflammation in mice. *Nat Immunol* 2005; 6:1047–53.
14 Al-Shami A, Spolski R, Kelly J *et al.* A role for TSLP in the development of inflammation in an asthma model. *J Exp Med* 2005; 202:829–39.
15 Seshasayee D, Lee WP, Zhou M *et al.* In vivo blockade of OX40 ligand inhibits thymic stromal lymphopoietin driven atopic inflammation. *J Clin Invest* 2007; 117:3868–78.
16 Bettelli E, Oukka M, Kuchroo VK. $T_H$-17 cells in the circle of immunity and autoimmunity. *Nat Immunol* 2007; 8:345–50.
17 Annunziato F, Cosmi L, Santarlasci V *et al.* Phenotypic and functional features of human Th17 cells. *J Exp Med* 2007; 20:1849–61.
18 Wilson NJ, Boniface K, Chan JR *et al.* Development, cytokine profile and function of human interleukin 17-producing helper T cells. *Nat Immunol* 2007; 8:950–7.
19 Manel N, Unutmaz D, Littman DR. The differentiation of human T(H)-17 cells requires transforming growth factor-β and induction of the nuclear receptor RORγt. *Nat Immunol* 2008; 9:641–9.
20 Volpe E, Servant N, Zollinger R *et al.* A critical function for transforming growth factor-β, interleukin 23 and proinflammatory cytokines in driving and modulating human $T_H$-17 responses. *Nat Immunol* 2008; 9:650–7.
21 Yang L, Anderson DE, Baecher-Allan C *et al.* IL-21 and TGF-β are required for differentiation of human T(H)17 cells. *Nature* 2008; 454:350–2.
22 Laurence A, O'Shea JJ. $T_H$-17 differentiation: of mice and men. *Nat Immunol* 2007; 8:903–5.
23 Molet S, Hamid Q, Davoine F *et al.* IL-17 is increased in asthmatic airways and induces human bronchial fibroblasts to produce cytokines. *J Allergy Clin Immunol* 2001; 108:430–8.
24 Chakir J, Shannon J, Molet S *et al.* Airway remodeling-associated mediators in moderate to severe asthma: effect of steroids on TGF-β, IL-11, IL-17, and type I and type III collagen expression. *J Allergy Clin Immunol* 2003; 111:1293–8.
25 Bullens DM, Truyen E, Coteur L *et al.* IL-17 mRNA in sputum of asthmatic patients: linking T cell driven inflammation and granulocytic influx? *Respir Res* 2006; 7:135.
26 Shannon J, Ernst P, Yamauchi Y *et al.* Differences in airway cytokine profile in severe asthma compared to moderate asthma. *Chest* 2008; 133:420–6.
27 Nicholson KG, Kent J, Ireland DC. Respiratory viruses and exacerbations of asthma in adults. *BMJ* 1993; 307:982–6.
28 Schaller M, Hogaboam CM, Lukacs N *et al.* Respiratory viral infections drive chemokine expression and exacerbate the asthmatic response. *J Allergy Clin Immunol* 2000; 118:295–302.
29 Falsey AR, Hennessey PA, Formica MA *et al.* Respiratory syncytial virus infection in elderly and high-risk adults. *N Engl J Med* 2005; 352:1749–59.
30 Greene CM, McElvaney NG. Toll-like receptor expression and function in airway epithelial cells. *Arch Immunol Ther Exp* 2005; 53:418–27.
31 Sha Q, Truong-Tran AQ, Plitt JR *et al.* Activation of airway epithelial cells by toll-like receptor agonists. *Am J Respir Cell Mol Biol* 2004; 31:358–64.
32 Kato A, Favoreto S Jr, Avila PC *et al.* TLR3- and Th2 cytokine-dependent production of thymic stromal lymphopoietin in human airway epithelial cells. *J Immunol* 2007; 179:1080–7.
33 Kadowaki N, Ho S, Antonenko S *et al.* Subsets of human dendritic cell precursors express different Toll-like receptors and respond to different microbial antigens. *J Exp Med* 2001; 194:863–9.

 

34 Watanabe N, Wang YH, Lee HK *et al.* Hassall's corpuscles instruct dendritic cells to induce $CD4^+CD25^+$ regulatory T cells in human thymus. *Nature* 2005; **436**:1181–5.
35 Watanabe N, Hanabuchi S, Soumelis V *et al.* Human thymic stromal lymphopoietin promotes dendritic cellmediated $CD4^+$ T cell homeostatic expansion. *Nat Immunol* 2004; 5:426–34.
36 Ho IC, Glimcher LH. Transcription: tantalizing times for T cells. *Cell* 2002; **109**:S109–20.
37 Rochman I, Watanabe N, Arima K *et al.* Direct action of thymic stromal lymphopoietin on activated human CD4+T cells. *J Immunol* 2007; **178**:6720–4.
38 Akamatsu T, Watanabe N, Kido M *et al.* Human TSLP directly enhances expansion of CD8+T cells. *Clin Exp Immunol* 2008; **154**:98–106.
39 Sallusto F, Lenig D, Förster R *et al.* Two subsets of memory T lymphocytes with distinct homing potentials and effector functions. *Nature* 1999; **401**:708–12.
40 Sallusto F, Geginat J, Lanzavecchia A. Central memory and effector memory T cell subsets: function, generation, and maintenance. *Annu Rev Immunol* 2004; **22**:745–63.
41 Campbell JJ, Murphy KE, Kunkel EJ *et al.* CCR7 expression and memory T cell diversity in humans. *J Immunol* 2001; **166**:877–84.
42 Rivino L, Messi M, Jarrossay D *et al.* Chemokine receptor expression identifies pre-T helper (Th)1, pre-Th2, and nonpolarized cells among human CD4+ central memory T cells. *J Exp Med* 2004; **200**:725–35.
43 Bratke K, Lommatzsch M, Julius P *et al.* Dendritic cell subsets in human bronchoalveolar lavage fluid after segmental allergen challenge. *Thorax* 2007; **62**:168–75.
44 Zuniga EI, McGavern DB, Pruneda-Paz JL *et al.* Bone marrow plasmacytoid dendritic cells can differentiate into myeloid dendritic cells upon virus infection. *Nat Immunol* 2004; 5:1227–34.

 

Clin J Gastroenterol (2009) 2:398–403
DOI 10.1007/s12328-009-0114-8

CASE REPORT

# Acute Epstein–Barr virus infection presenting as severe gastroenteritis without infectious mononucleosis-like manifestations

**Mikio Fujiwara · Shin'ichi Miyamoto · Kouta Iguchi · Toshihiro Matsunaka · Hiromi Sakashita · Tatsuaki Tsuruyama · Hirokazu Kanegane · Hiroyuki Marusawa · Hiroshi Nakase · Tsutomu Chiba**

Received: 22 May 2009 / Accepted: 7 September 2009 / Published online: 6 October 2009


**Abstract** Primary Epstein–Barr virus (EBV) infection is usually a self-limiting disease. Although it is sometimes accompanied by severe complications such as thrombocytopenia, hemolytic anemia, and splenic rupture, predominantly gastrointestinal complications are rarely reported. We studied an unusual case of primary EBV infection associated with severe hemorrhagic gastroenteritis. EBV infection was confirmed in the biopsy specimen by demonstrating the presence of EBV DNA by polymerase chain reaction, and of EBV-encoded small RNA (EBER)-positive cells by in-situ hybridization. Our patient was suspected of having primary EBV infection from the serological findings—EBV-viral capsid antigen IgM (+) and EBV nuclear antigen (−)—but he did not show typical clinical features of infectious mononucleosis such as lymph node swelling, pharyngitis, liver dysfunction, and splenomegaly. A definite diagnosis of primary EBV infection was made using biopsy specimens by demonstrating the presence of EBV DNA and EBER-positive cells.

M. Fujiwara · S. Miyamoto (✉) · K. Iguchi · T. Matsunaka · H. Marusawa · H. Nakase · T. Chiba
Department of Gastroenterology and Hepatology, Graduate School of Medicine, Kyoto University, 54 Shogoinkawaharacho, Sakyo-ku, Kyoto 606-8507, Japan
e-mail: shmiyamo@kuhp.kyoto-u.ac.jp

H. Sakashita · T. Tsuruyama
Laboratory of Diagnostic Pathology, Kyoto University Hospital, Kyoto, Japan

H. Kanegane
Department of Pediatrics, Graduate School of Medicine, Toyama University, Toyama, Japan

**Keywords** Epstein–Barr virus · Gastroenteritis · Polymerase chain reaction · EBV-encoded early small RNA

## Introduction

Epstein–Barr virus (EBV) is a very successful member of the herpesvirus family, infecting more than 90% of the world's adult population [1]. Like other herpesviruses, EBV is able to persist in the host for life. The primary infection usually occurs subclinically in childhood, however, some children or young adults manifest infectious mononucleosis (IM) with typical symptoms of fever, pharyngitis, lymphadenopathy, hepatosplenomegaly, and atypical lymphocytosis. EBV infects and immortalizes human B lymphocytes, and EBV-infected cells are targets of specific cytotoxic T lymphocytes [2]. IM is a self-limiting clinical syndrome that is occasionally compounded by rare severe complications involving the hematologic, neurological, renal, and respiratory systems [3–5]. However, a predominant gastrointestinal (GI) manifestation of primary EBV infection is rarely reported [6–9]. We successfully diagnosed this case of primary EBV infection of the GI tract by detecting EBV DNA and EBV-encoded small RNA (EBER) [10] using biopsy specimens in addition to the serological findings. This is the first report of primary EBV infection with an exclusive clinical manifestation of gastroenteritis in an immunocompetent adult.

## Case report

A 19-year-old man who presented with a 10-day history of fever (38°C), intermittent nausea, diarrhea, and persistent

lower-abdominal pain was admitted to a nearby hospital. He had no remarkable history of disease or medication including aspirin or nonsteroidal anti-inflammatory drugs. Physical examination revealed no abnormal findings such as lymphadenopathy or tonsillitis. He commenced hematemesis 7 days after admission despite relief of his gastrointestinal symptoms. Esophagogastroduodenoscopy (EGD) was performed. Endoscopic findings revealed diffuse reddish and edematous mucosa throughout the middle gastric body and the antrum (Fig. 1a, b). Biopsy specimens taken from the greater curvature of the middle body revealed atypical epithelial cells that were suspicious for adenocarcinoma. He was admitted to our hospital for further investigation. On admission, his body temperature was 38°C, blood pressure 110/62 mmHg, and pulse rate 92 beats/min. No skin rash, jaundice, or peripheral lymphadenopathy was observed. The abdomen was slightly distended with tenderness in the left upper quadrant, but neither liver nor spleen was palpable.

Laboratory examination was remarkable for a white blood cell count of 26200 cells/μl with 3.0% lymphocytes, no atypical lymphocytes, and C-reactive protein of 3.8 mg/dl. The peripheral blood hemoglobin was 7.7 g/dl. Protein-loss enteropathy was suggested by low albuminemia (2.2 g/dl) and hypogammaglobulinemia: IgG 396 (reference range 826–1840) mg/dl; IgA 78.3 (reference range 93–426) mg/dl; IgM 31.9 (reference range 27–205) mg/dl. Liver function tests were normal. Hepatitis B, hepatitis C, and human immunodeficiency virus were negative. General laboratory findings are shown in Table 1. EGD on the second day of hospitalization revealed a huge punched-out ulcer with white plaque on the greater curvature of the antrum (Fig. 1c), which differed from the previous findings. Multiple hemorrhagic duodenal ulcers were also observed (Fig. 1d). On the basis of these findings the patient was diagnosed with severe ischemic or infectious gastroenteritis of unknown etiology.

Hematochezia occurred suddenly on the sixth day of hospitalization. Rectosigmoidoscopy revealed a huge punched-out ulcer in the lower rectum (Fig. 1e). From these characteristic endoscopic findings, cytomegalovirus (CMV) infection was first suspected. However, both anti-CMV IgM and IgG were negative and neither CMV antigenemia nor CMV DNA was detected. Furthermore, CMV DNA was not detected by quantitative polymerase chain reaction (PCR) in the biopsy specimens from gastric and rectal lesions [11]. Bacterial cultures of the blood, urine, sputum, and stool were all negative and antibody titer to *Helicobacter pylori* was negative. On the other hand, EBV viral capsid antigen IgM was positive (2.4; normal <1.0), and EBV nuclear antigen was negative, suggesting a primary EBV infection. EBV DNA was detected by quantitative PCR in the biopsy specimen of the rectum (450 copies). Moreover, in situ hybridization (ISH) assay of EBER detected many EBER-positive cells in the biopsy specimens from gastric and rectal lesions. Taking these findings together, the patient was diagnosed with EBV-associated gastroenteropathy.

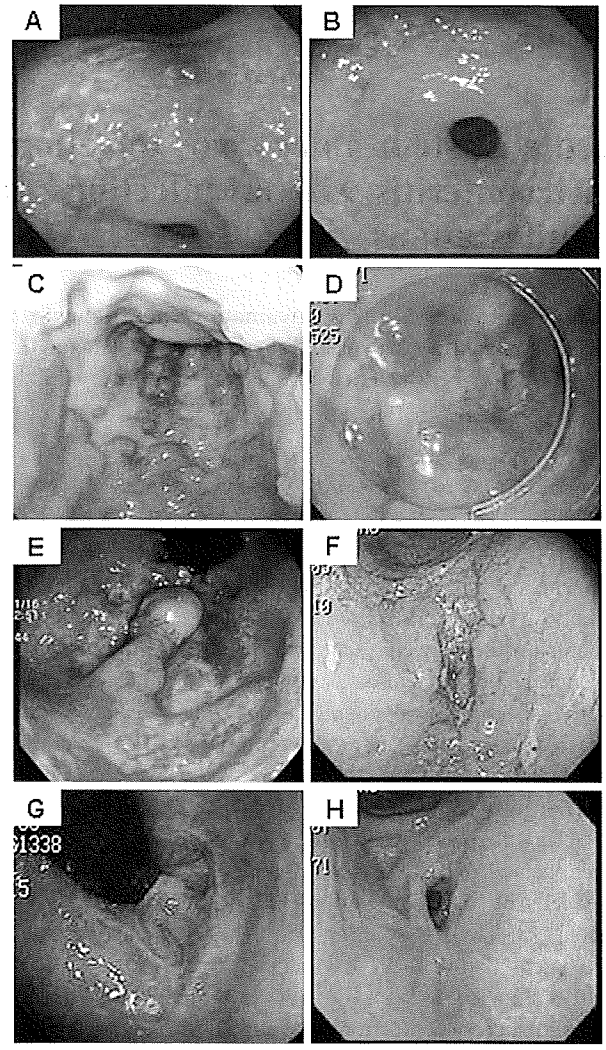


**Fig. 1** Changes in endoscopic findings. The first endoscopic findings (13 days before admission) revealed diffuse reddish and edematous mucosa throughout the middle gastric body (**a**) and the antrum (**b**). The second esophagogastroduodenoscopy (EGD; 2 days after admission) by our hospital revealed a huge punched-out ulcer with white plaque on the greater curvature of the antrum (**c**) and multiple hemorrhagic duodenal ulcers (**d**). Rectosigmoidoscopy (6 days after admission) showed a huge punched-out ulcer in the lower rectum (**e**). Follow-up EGD (27 days after admission) showed circumferential antral stenosis, though the mucosal lesions were greatly improved (**f**). Rectosigmoidoscopy (44 days after admission) demonstrated improvement of the rectal ulcer (**g**). After discharge, follow-up EGD was performed, showing no recurrence of gastric ulcer and improvement of the antral stenosis (**h**)

**Table 1** Laboratory data on admission

| Peripheral blood | Blood chemistry | Serological findings | Tumor markers | Viral markers |
|---|---|---|---|---|
| WBC 26200/μl | TP 4.3 g/dl | CRP 3.8 mg/dl | CEA 0.8 ng/ml | HBs Ag (−) |
| Seg 72% | ALB 2.2 g/dl | IgG 396 mg/dl | CA19-9 26.7 U/ml | HCV (−) |
| Band 23% | T-bil 0.3 mg/dl | IgA 78.3 mg/dl | AFP 1.5 ng/ml | CMV antigenemia (−) |
| Mono 2% | AST 20 IU/l | IgM 31.9 mg/dl | | HIV (−) |
| Lymph 3% | ALT 42 IU/l | | | |
| RBC 267 × $10^4$ | LDH 132 IU/l | | | |
| Hb 7.7 g/dl | ALP 313 IU/l | | | |
| Ht 23.7% | Cr 0.7 mg/dl | | | |
| Plt 88.9 × $10^4$/μl | BUN 18 mg/dl | | | |
| | Na 134 mEq/l | | | |
| | K 3.4 mEq/l | | | |
| | Cl 99 mEq/l | | | |
| | T-cho 103 mg/dl | | | |

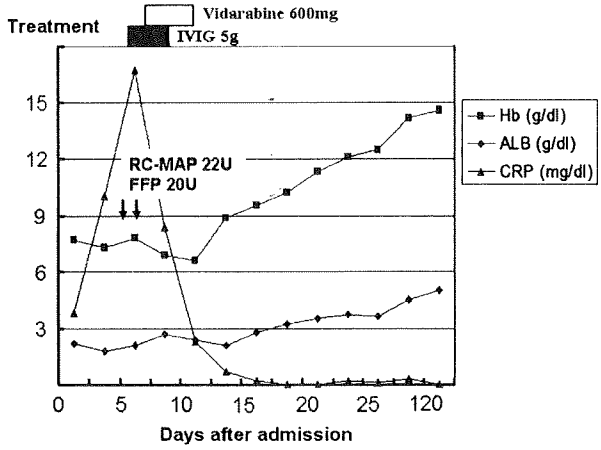


**Fig. 2** The clinical course of our patient. *Hb* Blood hemoglobin level, *ALB* albumin, *CRP* C-reactive protein, *IVIG* intravenous immunoglobulin, *RC-MAP* red cell concentrate in mannitol–adenine–phosphate solution, *FFP* fresh frozen plasma

Because his bloody stools continued to increase, rectosigmoidoscopy was again performed, demonstrating active bleeding from an exposed vessel, so endoscopic hemostasis by heat probe coagulation was performed. He received a blood transfusion, and vidarabine and intravenous immunoglobulin were administered for 8 and 5 days, respectively. After starting treatment, the patient's condition gradually improved. His clinical course is shown in Fig. 2, and changes in serological markers of EBV infection and immunoglobulin levels are shown in Table 2. Follow-up EGD on the 27th day of hospitalization showed severe antral stenosis because of a gastric ulcer scar on the greater curvature of the antrum (Fig. 1f). Biopsy specimens taken from the gastric ulcer scar revealed a remarkable decrease in EBER-positive cells. Endoscopic balloon dilatation was performed because of his stenotic symptoms. The patient's symptoms were relieved after balloon dilatation had been performed twice. Rectosigmoidoscopy on the 44th day of hospitalization revealed the complete disappearance of the rectal ulcer (Fig. 1g). Additionally, EBER-positive cells disappeared and EBV DNA was not detected in the biopsy specimens taken from the gastric and rectal lesions. He was discharged on the 63rd day of hospitalization. Six months later, follow-up EGD showed no antral obstruction (Fig. 1h). He is currently doing well 3 years later without recurrence of disease.

## Pathological findings

The first biopsy specimens from the gastric lesion revealed a severe structural atypia of the gastric gland ducts with mild nuclear atypia (Fig. 3a), suggestive of moderately differentiated tubular adenocarcinoma. However, a second set of biopsies of the gastric lesion revealed a prominent lymphoid infiltrate but no dysplastic lesion (Fig. 3b). Biopsy specimens from the rectal lesion also showed a marked infiltration of lymphocytes without dysplasia (Fig. 3c). Gastric and rectal biopsies did not detect intranuclear or cytoplasmic inclusion bodies in the epithelial cells. ISH assay of EBER revealed many EBER-positive cells in the biopsy specimens from gastric (Fig. 3d) and rectal lesions. Immunohistochemistry showed a large number of L26 (B cell)-positive and CD3 (T cell)-positive lymphocytes coexisting in the gastric and rectal lesions. Double labeling with EBER and cell-surface marker L26 (Fig. 3e) and CD3 (Fig. 3f) showed that both B and T cells were infected with EBV. Follow up EGD and rectosigmoidoscopy showed the disappearance of EBER-positive

**Table 2** Changes of serological markers of EBV infection and immunoglobulin levels during the clinical course

| Days after admission (discharge on day 63) | 4 | 32 | 60 | 116 | 494 |
|---|---|---|---|---|---|
| EBV-viral capsid antigen IgM (<1.0) | 2.4 (+) | 0.3 (−) | 0.2 (−) | 0.2 (−) | 0.5 (−) |
| EBV-viral capsid antigen IgG (<1.0) | 8.8 (+) | 9.0 (+) | 5.8 (+) | 6.0 (+) | 3.8 (+) |
| EB nuclear antigen (<10) | <10 | 20 | 20 | 20 | 40 |
| IgG (826–1840 mg/dl) | 396 | 669 | 581 | 812 | 549 |
| IgA (93–426 mg/dl) | 78 | 126 | 105 | 149 | 154 |
| IgM (27–205 mg/dl) | 32 | 114 | 115 | 149 | 91 |

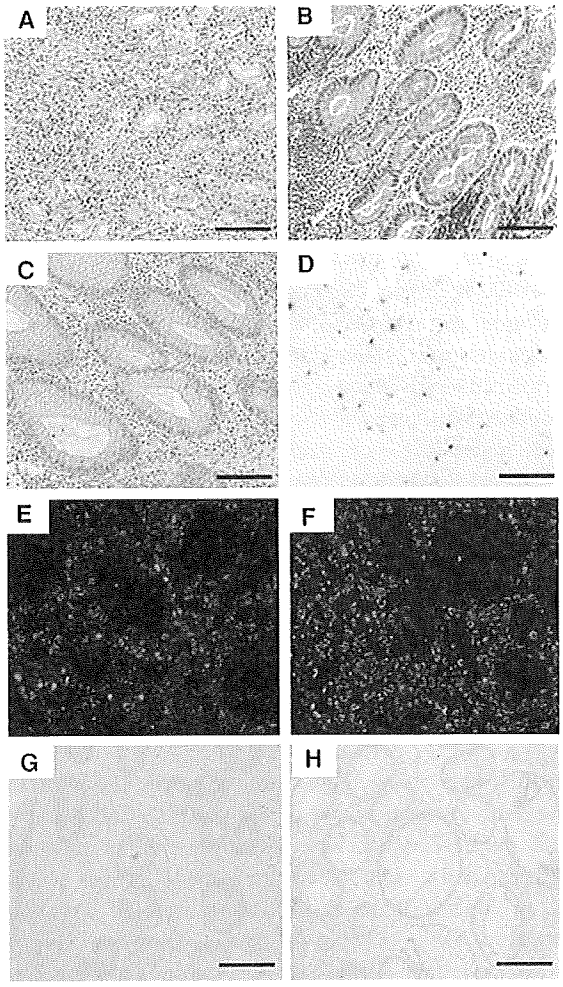


**Fig. 3** Histopathologic findings for the patient. A biopsy specimen taken from the erosive lesion of the greater curvature of the middle body showed severe structural atypia, but nuclear atypia was not observed (**a**). A hematoxylin–eosin (HE) stained biopsy specimen taken from the punched-out ulcer in the antrum (**b**) and lower rectal ulcer (**c**) showed marked infiltration of lymphocytes without dysplasia. In situ hybridization for EBV-encoded small RNA (EBER) (**d**) demonstrated positive nuclei of immune cells in the area corresponding to **b**. Double labeling with EBER and cell surface markers (L26 for B and CD3 for T lymphocytes) showed that EBER was positive in both B cells (**e**) and T cells (**f**). Follow up esophagogastroduodenoscopy and rectosigmoidoscopy showed the disappearance of EBER-positive cells in the biopsy specimens taken from the gastric (**g**) and rectal (**h**) lesions. *Scale bar* 200 μm

cells in the biopsy specimens taken from the gastric (Fig. 3g) and rectal lesions (Fig. 3h).

## Discussion

Clinical characteristics of published cases of primary EBV infection associated with gastroenteritis are summarized in Table 3. All cases were male and most cases showed some typical features of IM such as lymph node swelling, liver dysfunction, and splenomegaly. However, although the serological data in our patient strongly suggested a primary EBV infection, he did not show any typical clinical features of IM. Moreover, neither elevation of liver enzymes nor the appearance of atypical lymphocytes in the peripheral blood was observed during his clinical course. Thus, it was very difficult to confirm that the GI lesions in this case were because of the primary EBV infection.

Previous reports of endoscopic findings on EBV-associated GI lesions mainly documented erosions and ulcerations [6–9], but there are no characteristic endoscopic findings for EBV-associated GI lesions. Thus, it can be difficult to make a differential diagnosis particularly from gastric lymphoma.

Interestingly, we were able to follow the changes in the endoscopic appearance of the GI lesions in this case of primary EBV infection. The first endoscopic findings revealed only reddish mucosa and edema, but 15 days later the second endoscopy showed huge ulceration with surrounding multiple erosions in the antrum. These types of mucosal changes are often seen in active CMV infection [12], graft-versus-host disease [13] and vascular disease [14]. In our case, as CMV was not detected by any test, we performed quantitative PCR for EBV, using biopsy specimens to identify EBV DNA, and we confirmed the presence of EBV-infected cells by ISH for EBER. Thus, quantitative PCR for EBV DNA and ISH for EBER were both very useful for diagnosis of EBV-related gastroenteritis.

An important finding in this case is that ISH for EBER was positive in both B cells and T cells. It is well known that EBV mainly infects B cells but not T cells [3], but EBV infection of T cells is often associated with development of critical complications of IM, for example severe

**Table 3** Characteristics of EBV-related gastroenteritis in immunocompetent adults published in the literature

| | Age/ gender | Fever | Tonsillitis | LN swelling | Splenomegaly | Liver dysfunction | Atypical lymphocyte | GI symptom | Site of GI lesion | EBV-infected cell | Ref. |
|---|---|---|---|---|---|---|---|---|---|---|---|
| Case 1 | 40/male | + | – | + (paragastric) | + | – | + | Diarrhea | Stomach | B cell > T cell | [6] |
| Case 2 | 58/male | – | – | + (retroperitoneal) | + | + | – | Nausea/ Vomiting<br>Abdominal pain<br>Diarrhea | Stomach | B cell | [7] |
| Case 3 | 24/male | + | NS | + (mesenteric) | NS | ++ | NS | Hematochezia | Cecum | B cell/plasma cell | [8] |
| Case 4 | 59/male | + | – | + (gastrohepatic) | + | ++ | + | Nausea<br>Epigastralgia | Stomach | B cell/T cell | [9] |
| This case | 19/male | + | – | – | – | – | – | Nausea<br>Abdominal pain<br>Diarrhea<br>Hematochezia<br>Hematemesis | Stomach<br>Duodenum<br>Rectum | B cell/T cell | – |

*NS* not stated, *GI* gastrointestinal, *LN* lymph node

hepatitis [15] and EBV-associated hemophagocytic syndrome [16, 17]. Although in this case neither severe hepatitis nor EBV-associated hemophagocytosis occurred, EBV infection of T cells was associated with severe gastroenteritis.

X-linked lymphoproliferative syndrome (XLP) is a rare primary immunodeficiency disease characterized by an excessive response to EBV infection [18]. Major clinical phenotypes in XLP include severe fatal IM (60%), lymphoproliferative disorder (30%), and dysgammaglobulinemia (30%) [19]. The gene responsible for XLP has been identified as SH2D1A/DSHP/SLAM-associated protein (SAP). SAP comprises a single SH2 domain and a short carboxy-terminal tail, and it plays a critical role in signaling pathways involved in the development of a spectrum of immune responses [20]. To ascertain the possibility of XLP in this case, we investigated the membranous expression and mutations of SAP using peripheral T lymphocytes of the patient. Fluorescence-activated cell-sorter analysis and direct sequencing of SAP DNA revealed normal membranous expression of SAP and no mutation of the SAP gene.

There were 450 copies of EBV DNA per cell in the active stage of the rectal ulcer, which decreased to <10 copies after antiviral therapy. In previous published reports of primary EBV infection-associated gastroenteritis, with the exception of one case [8], the patients' symptoms and abnormal endoscopic findings resolved with only supportive treatment. Our case showed a severe course compared with previous cases. GI bleeding was stopped by endoscopic hemostasis and the patient's general condition was improved by intravenous supportive care including blood transfusion and infusion of vidarabine and immunoglobulin, but the efficacy of antiviral therapy was uncertain.

This case indicates that primary EBV infection can cause severe gastroenteritis in the absence of typical IM-like manifestations. Thus, when endoscopic examination reveals broad lesions with erosions and/or ulcerations of unknown etiology, primary EBV-associated GI disease should be considered as a differential diagnosis not only by clinicians but also by pathologists.

## References

1. Williams H, Crawford DH. Epstein–Barr virus: the impact of scientific advances on clinical practice. Blood. 2006;107:862–9.
2. Cohen JI. Epstein–Barr virus infection. N Engl J Med. 2000;343:481–92.
3. Okano M, Thiele GM, Davis JR, Grierson HL, Purtilo DT. Epstein–Barr virus and human diseases: recent advances in diagnosis. Clin Microbiol Rev. 1988;1:300–12.
4. Haller A, von Segesser L, Baumann PC, Krause M. Severe respiratory insufficiency complicating Epstein–Barr virus infection: case report and review. Clin Infect Dis. 1995;21:206–9.
5. Corssmit EP, Leverstein-van Hall MA, Portegies P, Bakker P. Severe neurological complications in association with Epstein–Barr virus infection. J Neurovirol. 1997;3:460–4.

6. Kitayama Y, Honda S, Sugimura H. Epstein–Barr virus-related gastric pseudolymphoma in infectious mononucleosis. Gastrointest Endosc. 2000;52:290–1.
7. Zhang Y, Molot R. Severe gastritis secondary to Epstein–Barr viral infection. Unusual presentation of infectious mononucleosis and associated diffuse lymphoid hyperplasia in gastric mucosa. Arch Pathol Lab Med. 2003;127:478–80.
8. Clayton RA, Malcomson RD, Gilmour HM, Crawford DH, Parks RW. Profuse gastrointestinal haemorrhage due to delayed primary Epstein–Barr virus infection in an immunocompetent adult. Histopathology. 2005;47:439–41.
9. Chen ZM, Shah R, Zuckerman GR, Wang HL. Epstein–Barr virus gastritis: an underrecognized form of severe gastritis simulating gastric lymphoma. Am J Surg Pathol. 2007;31:1446–51.
10. Shin SS, Berry GJ, Weiss LM. Infectious mononucleosis. Diagnosis by in situ hybridization in two cases with atypical features. Am J Surg Pathol. 1991;15:625–31.
11. Kou T, Nakase H, Tamaki H, Kudo T, Nishio A, Chiba T. Cytomegalovirus infection in patients with ulcerative colitis diagnosed by quantitative real-time PCR analysis. Dig Dis Sci. 2006;51:1052–5.
12. Goodgame RW. Gastrointestinal cytomegalovirus disease. Ann Intern Med. 1993;119:924–35.
13. Cruz-Correa M, Poonawala A, Abraham SC, Wu TT, Zahurak M, Vogelsang G, et al. Endoscopic findings predict the histologic diagnosis in gastrointestinal graft-versus-host disease. Endoscopy. 2002;34:808–13.
14. Geboes K, Dalle I. Vasculitis and the gastrointestinal tract. Acta Gastroenterol Belg. 2002;65:204–12.
15. Hara S, Hoshino Y, Naitou T, Nagano K, Iwai M, Suzuki K, et al. Association of virus infected-T cell in severe hepatitis caused by primary Epstein–Barr virus infection. J Clin Virol. 2006;35:250–6.
16. Kawaguchi H, Miyashita T, Herbst H, Niedobitek G, Asada M, Tsuchida M, et al. Epstein–Barr virus-infected T lymphocytes in Epstein–Barr virus-associated hemophagocytic syndrome. J Clin Invest. 1993;92:1444–50.
17. Su IJ, Chen RL, Lin DT, Lin KS, Chen CC. Epstein–Barr virus (EBV) infects T lymphocytes in childhood EBV-associated hemophagocytic syndrome in Taiwan. Am J Pathol. 1994;144:1219–25.
18. Purtilo DT, Cassel CK, Yang JP, Harper R. X-linked recessive progressive combined variable immunodeficiency (Duncan's disease). Lancet. 1975;1:935–40.
19. Hoshino T, Kanegane H, Doki N, Irisawa H, Sakura T, Nojima Y, et al. X-linked lymphoproliferative disease in an adult. Int J Hematol. 2005;82:55–8.
20. Nichols KE, Ma CS, Cannons JL, Schwartzberg PL, Tangye SG. Molecular and cellular pathogenesis of X-linked lymphoproliferative disease. Immunol Rev. 2005;203:180–99.

Original Paper

Digestion

Digestion 2010;81:193–203
DOI: 10.1159/000252790

Received: August 6, 2009
Accepted: October 13, 2009
Published online: January 19, 2010

# Celecoxib Inhibits CD133-Positive Cell Migration via Reduction of CCR2 in *Helicobacter pylori*-Infected Mongolian Gerbils

Seiji Futagami Tatsuhiko Hamamoto Mayumi Shimpuku Hiroyuki Nagoya Tetsuro Kawagoe Akane Horie Tomotaka Shindo Katya Gudis Choitsu Sakamoto

Department of Internal Medicine, Division of Gastroenterology, Nippon Medical School, Tokyo, Japan

**Key Words**

Celecoxib · CD133-positive cell migration · *Helicobacter pylori*-infected gerbils · Bone marrow-derived cells · *N*-Methyl-*N*-nitrosourea

**Abstract**

***Background/Aims:*** To see whether celecoxib prevents gastric cancer occurrence by disrupting the progression of chronic gastritis into gastric carcinoma through its inhibition of the migration of CD133-positive cells, one of the surface markers of bone marrow-derived cells, in *Helicobacter pylori*-infected gerbils. ***Methods:*** 70 gerbils were divided into six groups. Group 1 gerbils served as control (n = 6). 10 gerbils were given *N*-methyl-*N*-nitrosourea (MNU), 30 ppm (group 2). 6 short-term *Helicobacter pylori*-infected gerbils (group 3) were sacrificed after 8 weeks of *H. pylori* infection and 6 long-term *H. pylori*-infected gerbils were sacrificed after 42 weeks of *H. pylori* infection (group 4). 20 gerbils were given MNU pretreatment and long-term *H. pylori* infection (group 5). In addition, after *H. pylori* inoculation, 22 gerbils also received a celecoxib in their diet (group 6). CD133 and CCR2 expression in gastric tissues was evaluated by Western blot analysis and immunostaining. ***Results:*** CD133-positive cells were mainly localized in the bottom of the gastric epithelial cells. CD133-positive cells also migrated into gastric cancer tissues in this model. CD133-positive cells in MNU-pretreated *H. pylori*-infected gerbils were significantly increased compared to those in *H. pylori* short-term infected gerbils. Celecoxib treatment significantly reduced CD133-positive cell migration and CCR2 expression levels. CD133- and CCR2-positive cells were colocalized in *H. pylori*-infected gastritis and gastric cancer tissues. Celecoxib treatment significantly reduced the number of CD133- and CCR2-positive cells. ***Conclusions:*** Celecoxib inhibits CD133-positive cell migration via the reduction of CCR2 in this model. Further studies are needed to clarify the precise mechanisms driving *H. pylori* infection-induced CD133-positive cell migration and its link to the progression of chronic gastritis into gastric cancer.



## Introduction

The link between infection, chronic inflammation, and cancer has long been recognized, a prime example being infection with *Helicobacter pylori* and gastric cancer [1]. Chronic gastric inflammation, which develops as a consequence of *H. pylori*, leads over time to repetitive injury and repair resulting in hyperproliferation, an increased rate of mitotic error, and progression to adenocarcinoma. The same inflammatory environment that

KARGER

Fax +41 61 306 12 34
E-Mail karger@karger.ch
www.karger.com


0012–2823/10/0813–0193$26.00/0

Accessible online at:
www.karger.com/dig

Seiji Futagami, MD, PhD
Department of Internal Medicine, Division of Gastroenterology
Nippon Medical School
1-1-5 Sendagi, Bunkyo-ku, Tokyo 113-8602 (Japan)
Tel. +81 3 3822 2131, Fax +81 3 5685 1793, E-Mail seiji.futagami@gmail.com

favors the development of cancer has also been linked to homing and engraftment in peripheral tissue by bone marrow-derived cells (BMDCs). Recent studies suggest that BMDCs may possess an unexpected degree of plasticity and often home to sites of chronic injury or inflammation [2, 3]. BMDCs in both in vitro and in vivo models have been reported to migrate to sites of tissue damage [4]. Although the mechanism of subsequent BMDCs migration and differentiation is not established [5], it is clear that engrafting cells rely on external environmental cues for the orderly inactivation of growth programs and progression of appropriate differentiation [2, 3]. There is little information on the long-term consequences of recruiting pluripotent cells to areas of chronic inflammation where signals for cell growth and differentiation may be altered. Ponte et al. [6] have reported that BMDCs are able to migrate to a large set of chemotactic factors, including both growth factors and chemokines. Recently, Houghton et al. [7] have reported that BMDCs play an important role in the development of gastric cancers. However, there is no available data regarding the migration of BMDCs in gastric cancer tissues.

CD133, an antigenic marker for BMDCs containing hematopoietic stem cells [8], is expressed in several hematopoietic malignancies including acute myelogenous leukemia, acute lymphocytic leukemia, and myelodysplastic syndromes. Recent studies have reported that CD133 expression has also been identified as a cancer stem cell marker in brain, prostatic adenocarcinoma, colorectal cancers, and pancreatic cancers [9–11]. A high percentage of tumor samples was found to be positive for CD133 in gastric (47–55%), pancreatic (55–68%), and cholangiocarcinomas (67%, biliary type of liver cancer).

To investigate the mechanism of the recruitment of BMDCs in the metaplasia/dysplasia/carcinoma progression associated with chronic *H. pylori* infection, we used the established *H. pylori*-N-methyl-N-nitrosourea (MNU) treated Mongolian gerbil model. The present study was designed to see whether celecoxib prevents chronic gastritis from developing into gastric carcinoma in MNU-pretreated *H. pylori*-infected Mongolian gerbils through the suppression of CCR2 expression, that in turn suppresses the migration of CD133-positive cells.

## Methods

*Animals*

Seventy specific pathogen-free male Mongolian gerbils (5 weeks old, 40–45 g; Seac Yoshitomi, Fukuoka, Japan) were housed in steel cages on hard woodchip bedding in an air-conditioned biohazard room for infection programmed on a 12-hour light/12-hour dark cycle. They were given food (Oriental MF; Oriental Yeast, Tokyo, Japan) irradiated with 30 kGy γ-rays and autoclaved distilled water ad libitum.

*Bacterial Inoculation*

*H. pylori* (ATCC43504; CagA-positive, American Type Culture Collection, Rockville, Md., USA) were grown in *Brucella* broth (Becton Dickinson Co., Cockeysville, Md., USA) containing 10% v/v horse serum at 37°C under microaerobic conditions using Anaero Pack Campylo (Mitsubishi Gas Chemical Co., Inc., Tokyo, Japan) at high humidity for 40 h with shaking (150 rpm). Broth cultures were checked by phase-contrast microscopy for shape and mobility of *H. pylori*, and *Brucella* broth with $1 \times 10^9$ *H. pylori* colony-forming units (CFU) collected for administration to gerbils for groups 2 and 3.

*Chemicals*

MNU (Sigma, St. Louis, Mo., USA) was dissolved in distilled water at concentrations of 30 ppm and freshly prepared three times weekly. The solutions were given ad libitum as drinking water in light-shielded bottles to designated gerbils.

*Experimental Design*

The 70 gerbils were subdivided into six groups according to duration of *H. pylori* inoculation and MNU treatment as follows: group 1, control group (n = 6); group 2, MNU administration alone (n = 10); group 3, 8 weeks of *H. pylori* inoculation (n = 6); group 4, 42 weeks of *H. pylori* inoculation (n = 6); group 5, MNU pretreatment and 42 weeks of *H. pylori* inoculation (n = 20), and group 6, MNU pretreatment, 42 weeks of *H. pylori* inoculation and celecoxib (n = 22) (fig. 1). Groups 2, 5, and 6 gerbils were given 30-ppm MNU doses in their drinking water on odd-numbered weeks for a total 5-week exposure. On completion of MNU administration, the animals were given autoclaved distilled water for 1 week. After a 24-hour fast, all animals were given 0.8 ml *Brucella* broth with or without *H. pylori* through an oral catheter. Group 1 and 2 animals received *Brucella* broth without *H. pylori*, and groups 3–6 had *Brucella* broth with $1 \times 10^9$ *H. pylori* CFU. Six hours after inoculation, all animals were allowed free access to water and food. We had determined by preliminary testing that AB-PAS-positive cells did not appear prior to week 10 in *H. pylori*-infected gerbils pretreated with MNU. Thus, we initiated celecoxib therapy in group 6 gerbils 7 weeks after *H. pylori* inoculation, and continued this therapy for a period of 35 weeks until the end of trial (fig. 1). We chose a dose of 1,500 ppm celecoxib (Pfizer, New York, N.Y., USA) to be included in their CRF-1 diet (Oriental Yeast), as this has been shown to significantly reduce aberrant crypt foci in rats without inducing body weight loss [12]. Group 1, 2, 3, 4, 5, and 6 animals were maintained on basal CRF diet throughout the experiment. At experimental week 54, after a 24-hour fast, all animals were subjected to deep ether anesthesia, laparotomized, and their stomachs excised. The experimental protocol was approved by the Ethics Review Committee for Animal Experimentation of Nippon Medical School.

H. pylori *Detection*

To confirm *H. pylori* infection, gastric mucosal samples from the greater curvature were transferred into 1 ml sterile phosphate-buffered saline (PBS; 0.1 mol/l), and homogenized with 1 ml of

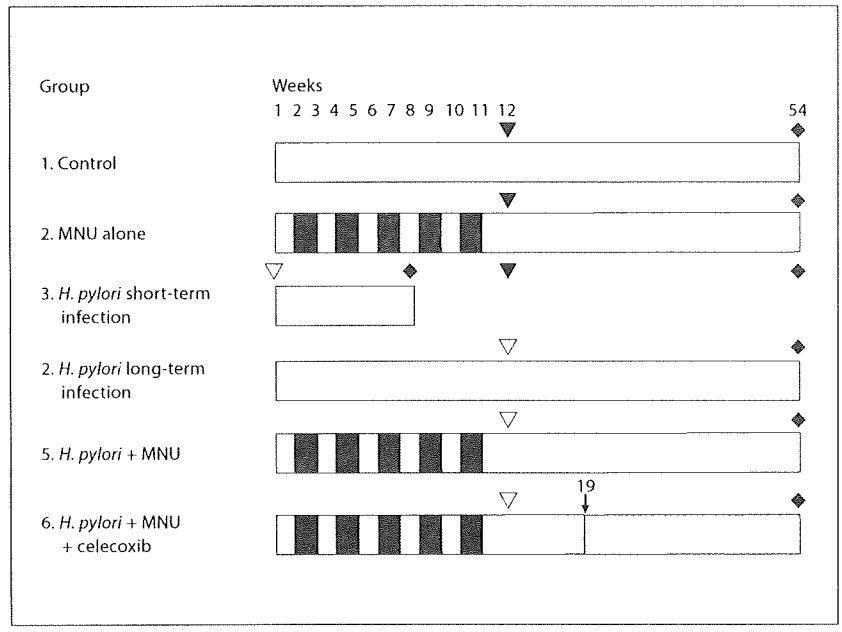


**Fig. 1.** Study protocols. 70 Mongolian gerbils were divided into six groups. Group 1 gerbils served as control (n = 6). 10 Mongolian gerbils were given five biweekly 30-ppm doses of MNU (group 2). 6 Mongolian gerbils were sacrificed after 8 weeks of short-term *H. pylori* infection (group 3). 6 Mongolian gerbils were exposed to 42 weeks of long-term *H. pylori* infection (group 4). 20 Mongolian gerbils were given five biweekly 30-ppm doses of MNU pretreatment and exposed to 42 weeks of long-term *H. pylori* infection (group 5). 22 Mongolian gerbils were allocated to group 6 for MNU pretreatment, 42 weeks *H. pylori* infection and celecoxib administration. Groups 1, 2, 4, 5, and 6 gerbils were sacrificed at week 54. ▽ = Inoculation with *H. pylori*, ▼ = inoculation with *Brucella* broth, ◆ = sacrifice of animals, ⇓ = initiation of celecoxib, ▨ = administration of celecoxib, ■ = MNU in drinking water at a concentration of 30 ppm on alternate weeks for groups 2, 5, and 6.

*Brucella* broth. Aliquots of 100 μl were inoculated on segregating agar plates for *H. pylori* (Eiken, Tokyo, Japan) and incubated at 37°C under microaerobic conditions for 6 days for culture of *H. pylori*.

*Histological Evaluation*

The excised stomachs were cut open along the greater curvature of the longitudinal axis and resected into nine strips; the strips were fixed in 4% paraformaldehyde in PBS, processed by standard methods, and embedded in paraffin. Tissues were sectioned at 5 μm for staining with HE staining and by immunohistochemistry for *H. pylori* (anti-*H. pylori* antibody; Dako, Copenhagen, Denmark). Adenocarcinomas of the glandular stomach were classified into *well differentiated lesions*, characterized by tubular structures with cellular atypia; *poorly differentiated tumors*, characterized by little tendency to form glandular structures with severe cellular atypia, and *signet ring cell carcinomas*, characterized by isolated tumor cells containing abundant amounts of mucin [13, 14]. To avoid counting reactive changes as neoplasms, well differentiated adenocarcinomas were diagnosed on the criterion of the presence of infiltration at least into the muscle layer. Heterotophic proliferative glands (HPG) localized beneath the muscularis mucosa were classified according to histological criteria [15]. Specimens were evaluated by two experienced pathologists in a blinded manner.

*Immunohistochemical Analysis of CD133 and CCR2*

For CD133 and CCR2 immunostaining in the gastric mucosa, 3-mm sections were deparaffinized and endogenous peroxidase activity blocked with 3% $H_2O_2$ in PBS. The samples were incubated overnight with anti-CCR2 antibody (diluted 1:250; Abcam, Inc., USA) or incubated 90 min with anti-CD133 antibody (diluted 1:100; Abcam, Inc.). After washing, bound antibody was detected using the LSAB 2 kit (Dako) with diaminobenzidine as the chromogen. As negative controls, primary antibodies were replaced with isotype-matched immunoglobulin. CCR2- and CD133-positive cells expression levels were determined by mean value of CCR2-positive or CD133-positive cell counts in four fields with ×400 magnification, respectively.

Double-labeling immunofluorescence methods and confocal laser scanning microscopy were used to evaluate the colocalization of immunoreactivity for the pair of goat anti-human CD133 (dilution 1:200, Abcam, Inc.) and rabbit anti-human CCR2 (dilution 1:1,000, Abcam, Inc.). The sections were incubated 60 min at room temperature with a mixture of the CCR2 and CD133 antibodies, and then with FITC or Texas red-conjugated secondary antibodies (mouse anti-rabbit IgG, dilution 1:400, Santa Cruz Biotechnology; donkey anti-goat IgG, dilution 1:400, Santa Cruz Biotechnology) followed by nuclear counterstaining with Mayer's hematoxylin for 2 min.

*Western Blot Analysis of CCR2 Expression Levels in Each Group*

Gastric tissues were disrupted by sonication in ice-cold 100 mmol/l Tris-HCl (pH 7.8) containing 1.0 mmol/l PMSF and 1.0 μmol/l pepstatin at 4°C. Equal amounts of protein (20 μg) were analyzed by SDS-PAGE and transferred onto nitrocellulose membranes. The membranes were blocked (5% non-fat dry milk in TBST) and incubated with anti-CCR2 antibody (diluted 1:100; Abcam, Inc.), or anti-β-actin (dilution 1:1,000, Amersham, Orsay, France) antibodies, and subsequently with peroxidase-conjugated secondary anti-rabbit antibody (Amersham). Detection by electrochemiluminescence was performed using Western blotting detection reagents (Amersham). Immunoblots were quanti-

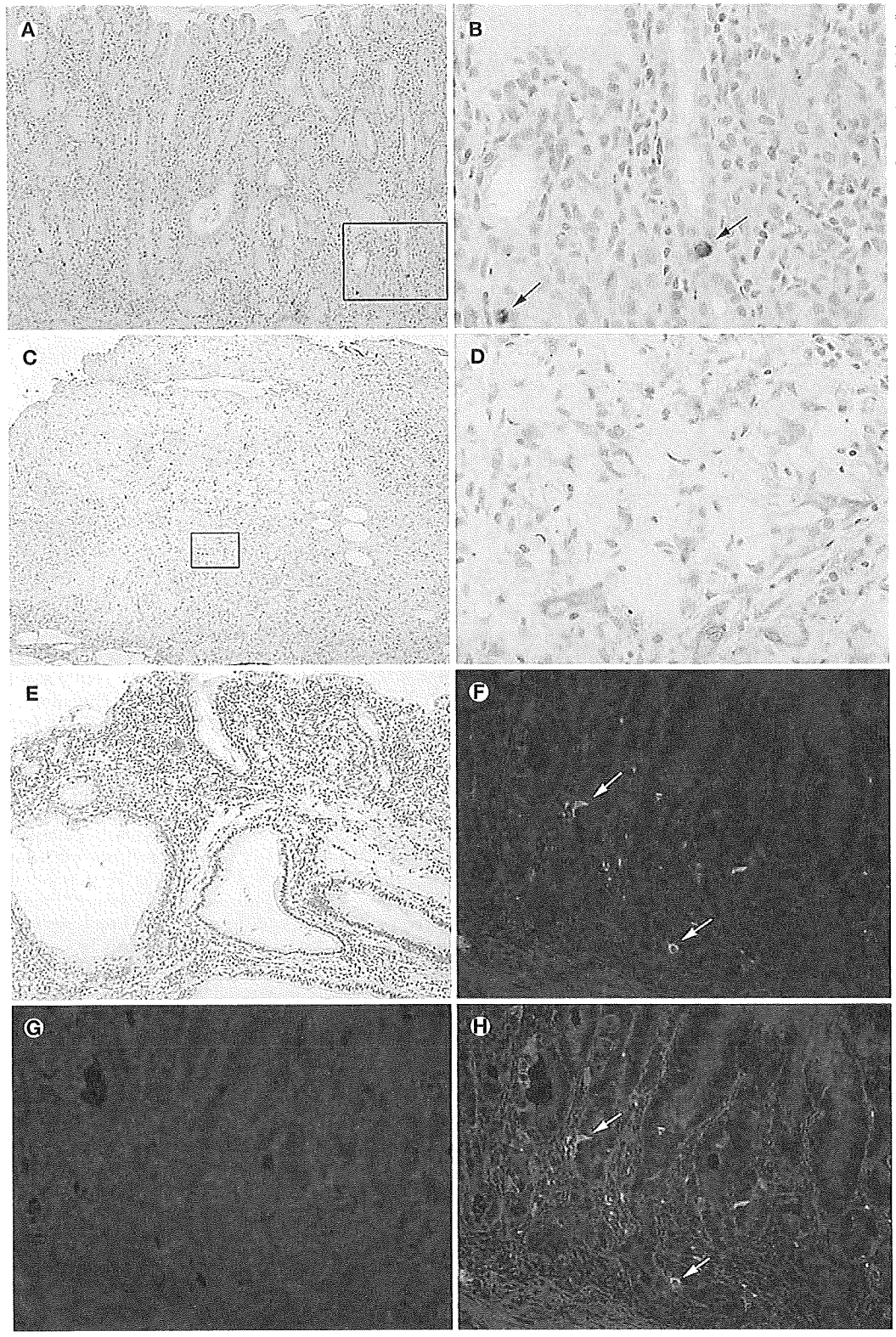


Color version available online

tatively analyzed by scanning the image and quantitating pixels using the Image Quant program.

*Statistical Analysis*

For statistical evaluation of data from each group, Student's t test for paired data and analysis of variance (ANOVA) for multiple comparisons were followed by Scheffé's test. The Mann-Whitney U test was used for analysis of categorical data. Fisher's exact test was used to assess differences in the incidence of gastric cancer among each group. $p < 0.05$ was considered statistically significant.

## Results

*Incidence of Gastric Adenocarcinoma in H. pylori-Infected Mongolian Gerbils*

Tumors were identified mostly in the pyloric mucosa adjacent to the fundic region. The incidence of tumors at sacrifice for group 1 was 0% (0/6), group 2, 0% (0/10), group 3, 0% (0/6), group 4, 0% (0/6), group 5, 65% (13/20), and group 6, 23% (5/22) (table 1).

*Localization of CD133-Positive Cells in H. pylori-Infected Mongolian Gerbils*

CD133-positive cells were mainly localized in the bottom of gastric epithelial cells (fig. 2A, B). CD133-positive cells also migrated into gastric cancer tissues in *H. pylori*-infected Mongolian gerbils (fig. 2C, D). In contrast, no CD133-positive cells were found in HPG lesions in *H. pylori*-infected Mongolian gerbils (fig. 2E). Figure 2F shows CD133 immunoreactivity in FITC-labeled (green) cells in MNU-pretreated *H. pylori*-infected gerbils. Figure 2G shows CD68-positive cells labeled with Texas red (red) for the same section. No CD133- and CD68-positive cells were found in the gastric epithelium of MNU-pretreated *H. pylori*-infected gerbils (fig. 2H) for the same section.

**Fig. 2.** Localization of CD133-positive cells in *H. pylori*-infected Mongolian gerbils. **A** Localization of CD133-positive cells in *H. pylori*-infected gerbils. **B** CD133-positive cells were mainly localized in the bottom of gastric epithelial cells (high magnification, ×400). **C** Localization of CD133-positive cells in gastric cancer tissues of MNU-pretreated *H. pylori*-infected gerbils. **D** Localization of CD133-positive cells in gastric cancer tissues (high magnification, ×450). **E** There was no CD133 expression in HPG lesions in *H. pylori*-infected gerbils. **F** CD133 immunoreactivity in MNU-pretreated *H. pylori*-infected gerbils. **G** CD68 immunoreactivity for the same section. **H** CD133 and CD68 did not coexpress in the same section.

**Table 1.** Incidence of gastric cancer in Mongolian gerbils (MGs)

| Group | Mongolian gerbil | Tumor-bearing MGs (%) |
|---|---|---|
| 1. Control | 6 | 0 (0) |
| 2. MNU alone | 10 | 0 (0) |
| 3. *H. pylori* short-term | 6 | 0 (0) |
| 4. *H. pylori* long-term | 6 | 0 (0) |
| 5. MNU + *H. pylori* | 20 | 13 (65) |
| 6. MNU + *H. pylori* + celecoxib | 22 | 5 (23)* |

* Significantly different from group 5; $p < 0.05$.

*Celecoxib Treatment Reduced CD133-Positive Cells in H. pylori-Infected Mongolian Gerbils*

There was no CD133 expression in the gastric tissue of MNU-pretreated gerbils (fig. 3Ai). There was a significant increase in CD133-positive cells in Mongolian gerbils subjected to long-term *H. pylori* infection (fig. 3Aii) but not in Mongolian gerbils undergoing short-term *H. pylori* infection. The increase in CD133-positive cells was also greater in MNU-pretreated *H. pylori*-infected gerbils than in gerbils subjected to short-term *H. pylori* infection, and was significant (fig. 3Aiii, Aiv). Interestingly, many CD133-positive cells could be seen beneath the mucosal muscularis of MNU-pretreated *H. pylori*-infected gerbils (fig. 3Aiv). Celecoxib treatment significantly reduced CD133-positive cell migration into the gastric mucosa of MNU-pretreated *H. pylori*-infected gerbils (fig. 3Av, B).

*CCR2 Expression Levels in Each Group*

Since celecoxib treatment reduced CCR2 immunoreactivity in gastric tissue, we evaluated the effect of celecoxib on CCR2 expression levels by Western blot analysis. CCR2 expression levels in long-term *H. pylori*-infected gerbils and MNU-pretreated *H. pylori*-infected gerbils were significantly higher than in MNU-alone gerbils (fig. 4A, B); while continuous celecoxib treatment significantly reduced CCR2 expression levels in MNU-pretreated *H. pylori*-infected gerbils down to one fifth its original levels (fig. 4A, B).

*Localization of CD133 and CCR2 Expression in H. pylori-Infected Mongolian Gerbils*

To investigate whether CD133-positive cells migrate into *H. pylori*-infected gastritis mucosa and gastric cancer tissues via CCR2 expression, we conducted double staining analysis using anti-CD133 antibody and anti-CCR2

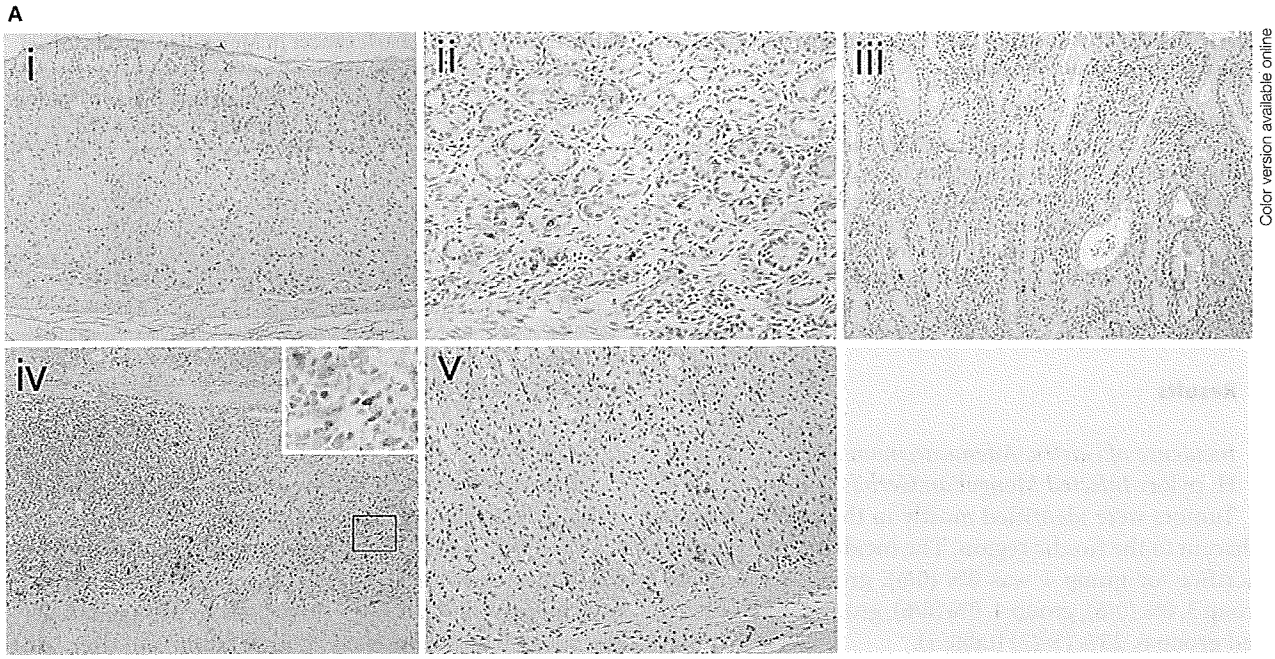


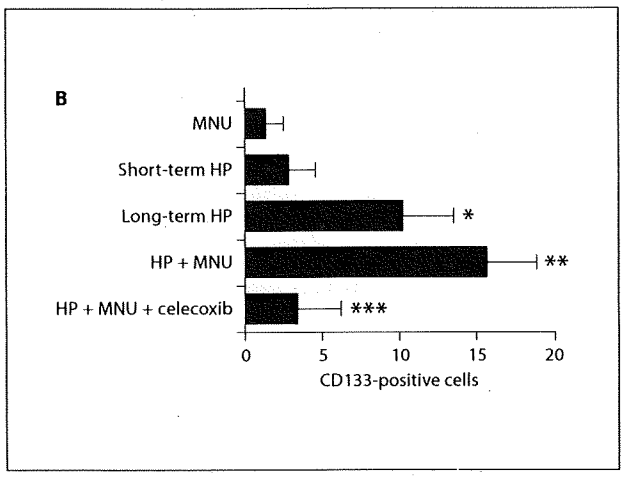


**Fig. 3.** CD133-positive cell numbers in each group. **A** (i) There was no CD133 expression in the gastric tissue of MNU-treated gerbils. (ii) CD133-positive cells could be seen in long-term *H. pylori*-infected gerbils. (iii) Many CD133-positive cells could be seen in MNU-pretreated *H. pylori*-infected gerbils. (iv) Many CD133-positive cells migrated beneath the muscularis mucosa in MNU-pretreated *H. pylori*-infected gerbils. Right window: high magnification (×400). (v) A few CD133-positive cells were localized in the gastric tissue of celecoxib-treated gerbils. **B** There was a significant increase (* $p < 0.05$) in the number of CD133-positive cells in the gastric tissue of long-term *H. pylori*-infected gerbils, over that of short-term *H. pylori*-infected gerbils. There was also a significant increase (** $p < 0.05$) in the number of CD133-positive cells in the gastric tissue of MNU-pretreated gerbils infected with *H. pylori*, over that in short-term *H. pylori*-infected gerbils. Celecoxib treatment significantly (*** $p < 0.05$) inhibited CD133-positive cell migration into the gastric tissue of MNU-pretreated *H. pylori*-infected gerbils.

antibody. Figure 5A shows CD133 immunoreactivity in FITC-labeled (green) cells in MNU-pretreated *H. pylori*-infected gerbils. Figure 5B shows CCR2-positive cells labeled with Texas red (red) for the same section. CD133 and CCR2 expression colocalized in the gastric epithelium of MNU-pretreated *H. pylori*-infected gastritis (yellow) for the same section (fig. 5C). Figure 5E shows CD133 immunoreactivity in FITC-labeled (green) cells in gastric cancer tissues. Figure 5F shows CCR2-positive cells labeled with Texas red (red) for the same section. CD133- and CCR2-positive cells colocalized in gastric cancer tissues (yellow) (fig. 5G). To investigate whether celecoxib could inhibit the migration of CD133-positive cells via CCR2 expression, we evaluated CD133- and CCR2-positive cell numbers in MNU-pretreated *H. pylori*-infected gerbils with or without celecoxib treatment. There was a significant increase in the number of CD133- and CCR2-positive cells in MNU-pretreated *H. pylori*-infected gerbils compared to gerbils exposed only to MNU (fig. 6). In addition, celecoxib treatment significantly reduced the number of CD133- and CCR2-positive cells in MNU-pretreated *H. pylori*-infected gerbils (fig. 6).

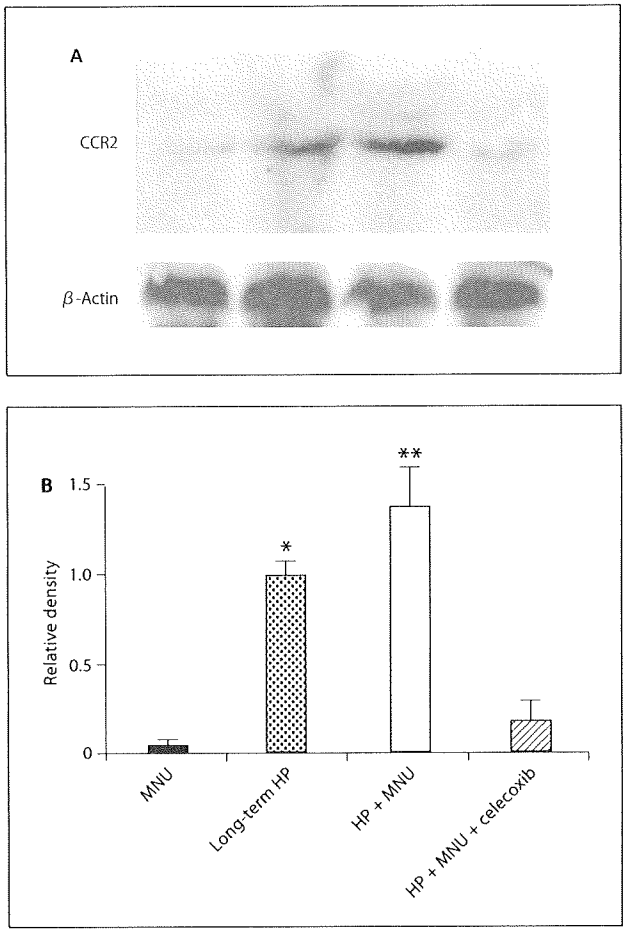


**Fig. 4.** CCR2 expression levels in *H. pylori*-infected gerbils. **A** Representative Western blots of gastric tissues from MNU-pretreated *H. pylori*-infected gerbils for CCR2 and β-actin. MNU = MNU-alone gerbils; Long-term HP = long-term *H. pylori*-infected gerbils; HP+MNU = MNU-pretreated *H. pylori*-infected gerbils; HP+MNU+celecoxib = celecoxib-treated gerbils. **B** Quantitation of CCR2 expression relative to β-actin expression was determined by densitometric analysis of each group using six separate experiments. Data are the mean ± SE. * $p < 0.05$ vs. HP+MNU+celecoxib and MNU alone, ** $p < 0.05$ vs. HP+MNU+celecoxib and MNU alone, respectively.

## Discussion

In this study, we investigated whether a selective COX-2 inhibitor, celecoxib, could inhibit the incidence of gastric adenocarcinoma in *H. pylori*-infected Mongolian gerbils through the suppression of CD133-positive cell migration into gastric tissue. Our major findings are: (1) CD133-positive cells in MNU-pretreated *H. pylori*-infected gerbils were significantly increased compared to *H. pylori* short-term infected gerbils. (2) CD133-positive cells could be seen in the bottom of gastric epithelium of *H. pylori*-infected gastritis and gastric cancer tissues in this model. (3) Celecoxib treatment significantly inhibited CD133- and CCR2-positive cell count in MNU-pretreated *H. pylori*-infected gerbils.

Previous research suggests that BMDCs play an important role in the development of gastric cancers [7]. This study primarily emphasizes the importance of chronic inflammation in recruiting BMDCs. The contribution of BMDCs to the neointimal lesion has been described, however, characterization of the progenitor cell remains controversial. Unfortunately, purification of solid tumor-initiating cells such as gastric cancer has been difficult because of the paucity of cell surface markers that enable cell sorting. CD133-positive cells are also expressed in hematologic, neuronal, and endothelial progenitor cells [16–18]. Therefore, CD133 has been suggested as one of the surface markers for BMDCs containing hematopoietic stem cells [8, 19]. We are the first to report that CD133-positive cells migrate into gastric cancer tissues in *H. pylori*-infected animal models. In contrast, many studies have proposed that CD133-positive cells are also markers of tumor-initiating cells in diverse organs such as prostate, pancreas, and colon cancer. In human gastric cancers, Smith et al. [20] have reported that CD133-positive cells were detected in gastric cancer tissues. However, there is no available data about the precise role in CD133-positive cells in gastric cancer tissues. Further studies are needed to clarify whether CD133-positive cells are derived from bone marrow using a same-slide technique of staining for CD133-positive cells, X chromosomes and Y chromosomes using a bone marrow-transplanted gerbil model as well as in previous studies [7]. Although recent investigations have demonstrated that BMDCs could contribute to cancers of the small intestine, colon, lung [21], larynx, and brain [22], it is yet to be determined whether cancers originating from BMDCs in fact exist.

BMDCs have been reported to migrate to sites of tissue damage in both in vitro and in vivo models [4]. Although the migratory behavior of BMDCs has now been extensively documented, the distinct signals that guide the migration of BMDCs to specific in vivo targets are unknown. Chemotactic cytokines have been implicated in controlling BMDCs migration into tumors. Ritter et al. [23] have also reported that breast cancer cell-derived FGF2 and VEGF are chemoattractants for BMDCs. Widera et al. [24] have reported that MCP-1 is a major

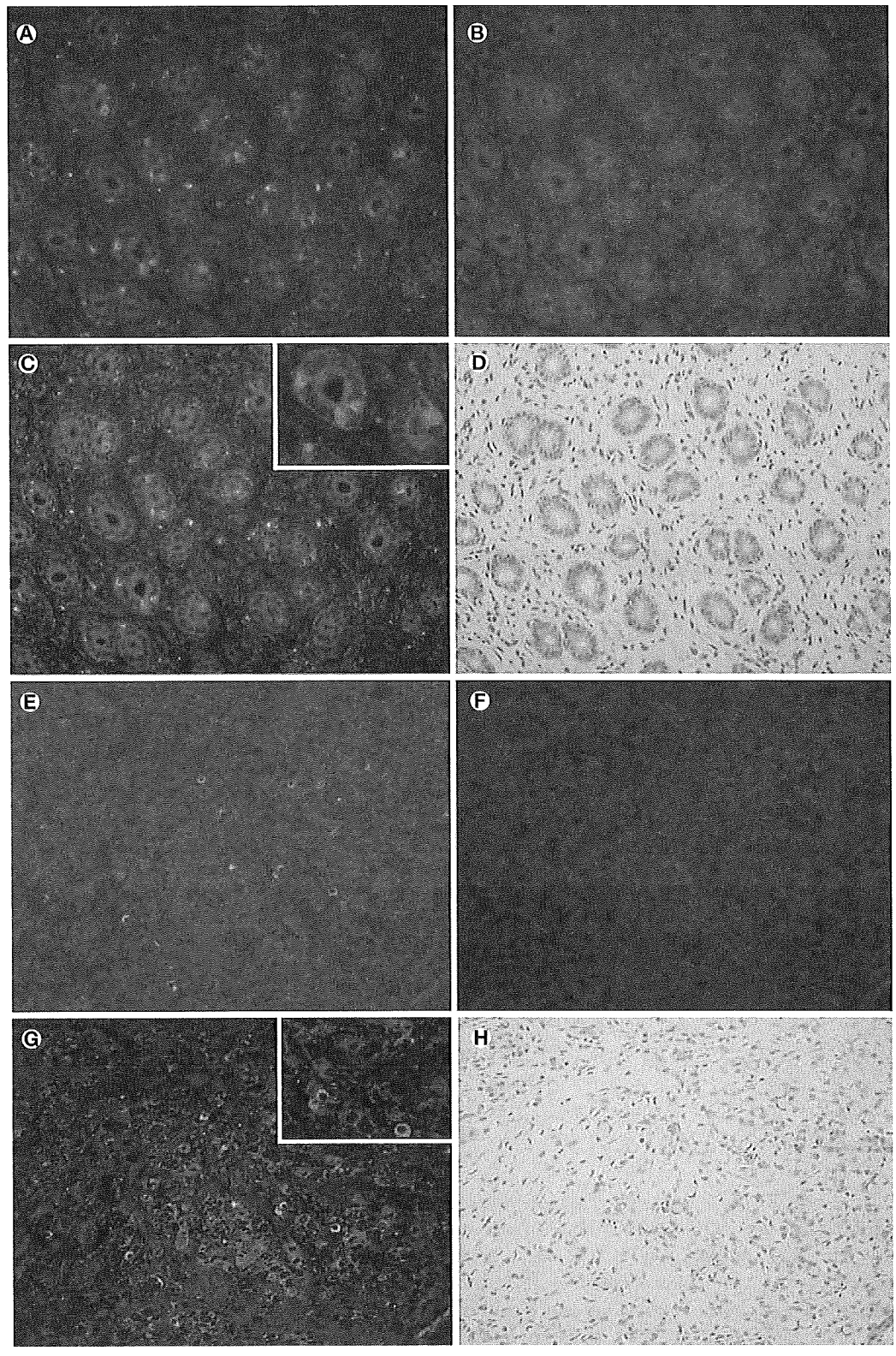


Color version available online

5

chemotactic factor for neural stem cells. Zhang et al. [25] have reported that treatment with an MCP-1 neutralizing antibody prevented bone marrow-derived microglia infiltration into the spinal cord after nerve injury. Belema-Bedada et al. [26] have also reported that CCR2 is necessary for organ-specific homing of BMDCs into hearts damaged by ischemia/reperfusion. In addition, Ito et al. [27] have also reported that CCR2 in bone marrow cells plays an important role in the recruitment of macrophages into obese adipose tissue. Thus, MCP-1/CCR2 appears to be an important factor in the migration of BMDCs [27]. In this study, we are the first to report that a marker for BMDCs, CD133-positive cells, migrated into *H. pylori*-infected gastritis and gastric cancer tissues, and that CD133-positive cells coexpressed with CCR2 expression in our model. We have previously reported that MCP-1 was expressed in *H. pylori*-infected gastritis and gastric cancer tissues [28, 29]. MCP-1 derived from *H. pylori*-infected gastritis and gastric cancer might stimulate the migration of CD133- and CCR2-double-positive cells in this model. Further study is warranted to determine the contribution of CD133 and CCR2 coexpression in the development of gastric cancer. In our study, CD133-positive cells in long-term *H. pylori*-infected gerbils significantly increased over short-term *H. pylori*-infected gerbils. Previous studies have reported that, in models in which parietal cells were ablated with DMP777, a protonophore with specificity for parietal cell acid-secretory membranes, parietal cell mass was reestablished using host cells and was not of bone marrow origin [7]. These reports and our results suggest that chronic infection and inflammation were necessary for repopulation of gastric epithelium with BMDCs. Further studies are needed to clarify what kinds of cytokines and growth factors affect the accumulation of BMDCs, including CD133-positive cells in this model.

**Fig. 5.** CD133 and CCR2 colocalization in *H. pylori*-infected gerbils. **A** CD133 immunoreactivity in the gastric mucosa of MNU-pretreated *H. pylori*-infected gerbils. **B** CCR2 immunoreactivity in the gastric mucosa for the same section. **C** CD133- and CCR2-positive cells in the same section. Right window: high magnification (×400). **D** Meyer's hematoxylin staining in the same section. **E** CD133 immunoreactivity in gastric cancer tissues of MNU-pretreated *H. pylori*-infected gerbils. **F** CCR2 immunoreactivity in the same section. **G** CD133- and CCR2-positive cells for the same section. Right window: high magnification (×400). **H** Meyer's hematoxylin staining in the same section.

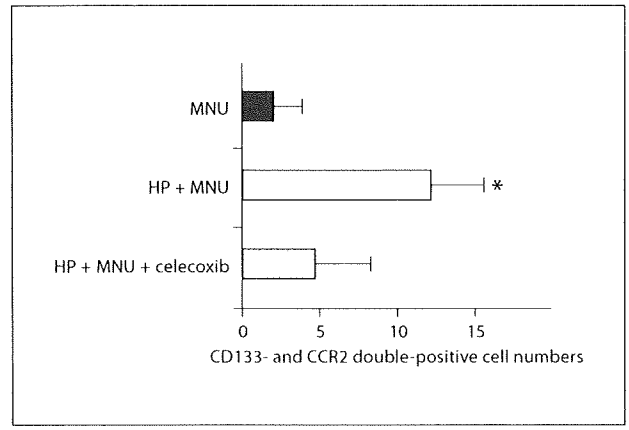


**Fig. 6.** CD133 and CCR2 double-positive cell numbers in each group. CD133 and CCR2 double-positive cell numbers in MNU-pretreated *H. pylori*-infected gerbils significantly (* $p < 0.05$) increased over those of gerbils treated only with MNU. Celecoxib treatment significantly (* $p < 0.05$) reduced CD133 and CCR2 double-positive cell numbers in MNU-pretreated *H. pylori*-infected gerbils.

Selective COX-2 inhibitors have been reported to inhibit tumor development in animal and human studies [30, 31]. Celecoxib has been also shown to reduce *N*-methyl-*N'*-nitro-*N*-nitrosoguanidine-induced gastric cancer incidence in rats [32] and *H. pylori*-infected Mongolian gerbils [33]. Although the inhibitory effect of a selective COX-2 inhibitor on the development of gastric cancer has already been reported in *H. pylori*-infected animal models, the events or processes prevented by COX-2 inhibition, that is, the progression of gastritis into cancer has yet to be elucidated. We are the first to report that celecoxib significantly reduced the migration of CD133-positive cells into *H. pylori*-infected mucosa. We have reported that CCR2 expression in endothelial cells and macrophages was dependent on COX-2-derived PGE2 production [34]. Liang et al. [35] have also reported that a selective COX-2 inhibitor, celecoxib-reduced CCR2 mRNA expression and skin damage after radiation. Our results and previous studies suggest that celecoxib might significantly suppress the migration of CD133-positive cells in *H. pylori*-infected Mongolian gerbils via the reduction of CCR2 expression levels. Further studies are clearly needed to clarify the precise mechanism driving the inhibition of CD133-positive cell migration by celecoxib. Such studies should take a closer look at the role of PGE2 in the suppression of CCR2 expression levels and the migration of CD133-positive cells.